0026-895X/02/6203-756–761$7.00
MOLECULAR PHARMACOLOGY
Copyright © 2002 The American Society for Pharmacology and Experimental Therapeutics
Mol Pharmacol 62:756–761, 2002

Vol. 62, No. 3
1777/1008459
Printed in U.S.A.

Effects of Phosphoinositide 3-Kinase on the Endothelin-1–Induced Activation of Voltage-Independent Ca^{2+} Channels and Mitogenesis in Chinese Hamster Ovary Cells Stably Expressing Endothelin$_A$ Receptor

YOSHIFUMI KAWANABE, NOBUO HASHIMOTO, and TOMOH MASAKI

Departments of Neurosurgery (Y.K., N.H.) and Pharmacology (Y.K., T.M.), Kyoto University Faculty of Medicine, Kyoto, Japan

Received April 5, 2002; accepted June 18, 2002

This article is available online at http://molpharm.aspetjournals.org

ABSTRACT

We recently demonstrated that endothelin-1 (ET-1) activates two types of Ca^{2+}-permeable nonselective cation channel (designated NSCC-1 and NSCC-2) and a store-operated Ca^{2+} channel (SOCC) in Chinese hamster ovary cells expressing endothelin$_A$ receptor (CHO-ET$_A$R). In addition, these channels can be discriminated using Ca^{2+} channel blockers (*R*,*S*)-(3,4-dihydro-6,7-dimethoxy-isochinolin-1-yl)-2-phenyl-*N*,*N*-di[2-(2,3,4-trimethoxyphenyl)ethyl]acetamid mesylate (LOE 908) and 1-(β-[3-(4-methoxyphenyl)propoxy]-4-methoxyphenethyl)-1*H*-imidazole (SK&F 96365). LOE 908 is a blocker of NSCC-1 and NSCC-2, whereas SK&F 96365 is a blocker of SOCC and NSCC-2. In this study, we investigated the effects of phosphoinositide 3-kinase (PI3K) on the ET-1–induced activation of these channels and mitogenesis in CHO-ET$_A$R using wortmannin and 2-(4-morpholinyl)-8-phenyl-4H-1-benzopyran-4-one (LY 294002), inhibitors of phosphoinositide 3-kinase (PI3K). ET-1–induced Ca^{2+} influx was partially inhibited in CHO-ET$_A$R pretreated with wortmannin or LY 294002. In contrast, addition of wortmannin or LY 294002 after stimulation with ET-1 did not suppress Ca^{2+} influx. The Ca^{2+} channels activated by ET-1 in wortmannin or LY 294002-treated CHO-ET$_A$R were sensitive to LOE 908 and resistant to SK&F 96365. Wortmannin also partially inhibited ET-1–induced mitogenesis. LOE 908, but not SK&F 96365, abolished the wortmannin-resistant part of mitogenesis. The IC_{50} values (~30 nM) of wortmannin for the ET-1–induced Ca^{2+} influx and mitogenesis were similar to those for the ET-1-induced PI3K activation. In conclusion, NSCC-2 and SOCC are stimulated by ET-1 via PI3K-dependent cascade, whereas NSCC-1 is stimulated via PI3K-independent cascade. Moreover, PI3K seems to be required for the activation of the Ca^{2+} entry, but not for its maintenance. In addition, PI3K is involved in the ET-1–induced mitogenesis that depends on the extracellular Ca^{2+} influx through SOCC and NSCC-2.

Endothelin-1 (ET-1) was discovered as a potent vasoconstricting peptide secreted from endothelial cells (Yanagisawa et al., 1988). It is generally accepted that ET-1 may play a role in the pathogenesis of certain clinical conditions, such as hyperlipoproteinemia, atherosclerosis, stroke, cerebral vasospasm, and tumor growth (Lerman et al., 1991; Haak et al., 1994). Moreover, recent reports showed that the extracellular Ca^{2+} influx is required for ET-1–induced vascular contraction and mitogenesis (Zhang et al., 1999; Kawanabe et al., 2002a). These results indicate that if the activation pathways of Ca^{2+} channels involved in the extracellular Ca^{2+} influx caused by ET-1 are revealed, blockade of these pathways may become a new treatment for ET-1–induced clinical conditions described above. We recently demonstrated that the sustained increase in intracellular free Ca^{2+} concentration ($[Ca^{2+}]_i$) caused by ET-1 results from Ca^{2+} entry through three types of VICC in CHO cells stably expressing human endothelin$_A$ receptors (CHO-ET$_A$R), two types of Ca^{2+}-permeable nonselective cation channel (designated NSCC-1 and NSCC-2), and a store-operated Ca^{2+} channel (SOCC) (Kawanabe et al., 2001). Importantly, these channels can be distinguished in terms of the sensitivity to Ca^{2+} channel blockers SK&F 96365 and LOE 908. NSCC-1 is sensitive to LOE 908 and resistant to SK&F 96365; NSCC-2

This work was supported by Grants-in-Aid from the Ministry of Education, Science, Sports and Culture of Japan, by a grant from the Smoking Research Foundation, Japan, and by the Uehara Memorial Foundation Fellowship, Tokyo, Japan.

ABBREVIATIONS: ET-1, endothelin-1; $[Ca^{2+}]_i$, intracellular free Ca^{2+} concentration; CHO, Chinese hamster ovary; ET$_A$R, human endothelin$_A$ receptor; VICC, voltage-independent Ca^{2+} channel; NSCC, nonselective cation channel; SOCC, store-operated Ca^{2+} channel; SK&F 96365, 1-(β-[3-(4-methoxyphenyl)propoxy]-4-methoxyphenethyl)-1*H*-imidazole; LOE 908, (*R*,*S*)-(3,4-dihydro-6,7-dimethoxy-isochinolin-1-yl)-2-phenyl-*N*,*N*-di[2-(2,3,4-trimethoxyphenyl)ethyl]acetamid mesylate; PLC, phospholipase C; PI3K, phosphoinositide 3-kinase; MTT, 3-(4,5-dimethyl-2-thiazolyl)-2,5-diphenyl tetrazolium bromide; LY 294002, 2-(4-morpholinyl)-8-phenyl-4H-1-benzopyran-4-one.

is sensitive to both LOE 908 and SK&F 96365; and SOCC is resistant to LOE 908 but sensitive to SK&F 96365 (Kawanabe et al., 2001). VICCs activated by ET-1 in CHO-ET_AR seem to be pharmacologically similar to those in vascular smooth muscle cells, which predominantly express ET_ARs (Kawanabe et al., 2002a). Therefore, our findings on CHO cells may give some insights into the functional roles of ET_ARs related to ET-1–induced Ca^{2+} channel activation on vascular smooth muscle cells.

The types of G_α protein involved in activation of NSCC-1, NSCC-2, and SOCC are different in CHO-ET_AR. NSCC-1 is activated via a G_{12}-dependent pathway, NSCC-2 is activated via both a G_q/phospholipase C (PLC)- and a G_{12}-dependent pathway, and SOCC is activated via a G_q/PLC-dependent pathway (Kawanabe et al., 2002c). However, less is known about intracellular signaling pathways regulate the activation of these Ca^{2+} channels. Previous reports demonstrate that phosphoinositide 3-kinase (PI3K) plays important roles for stimulation of L-type voltage-dependent Ca^{2+} channels by angiotensin (Seki et al., 1999; Viard et al., 1999) and T-cell Ca^{2+} signaling via phosphatidylinositol 3,4,5-triphosphate-sensitive Ca^{2+} entry pathway (Hsu et al., 2000). ET-1 activates PI3K in CHO-ET_AR from the data using the PI3K inhibitor wortmannin (Sugawara et al., 1996). Therefore, at first, we examined whether and which VICCs are activated by ET-1 in CHO-ET_AR via PI3K-dependent pathway.

ET-1 induces mitogenic response in CHO-ET_AR (Sugawara et al., 1996). However, it remains unclear whether Ca^{2+} influx is essential for ET-1–induced mitogenesis of CHO-ET_AR, and it is equally unclear what types of Ca^{2+} channels are involved in mitogenesis in CHO-ET_AR. We attempted to pharmacologically characterize the Ca^{2+} channels involved in ET-1–induced mitogenesis in CHO-ET_AR using SK&F 96365 and LOE 908. We also investigated the effects of PI3K on the ET-1–induced mitogenesis that depends on extracellular Ca^{2+} influx.

Materials and Methods

Cell Culture. Stable expression of ET_ARs in CHO cells was accomplished as described previously (Kawanabe et al., 2001). CHO-ET_AR were routinely maintained in Ham's F12 medium supplemented with 10% fetal calf serum under a humidified atmosphere of 5% CO_2/95% air.

Monitoring of $[Ca^{2+}]_i$ in CHO-ET_AR. The $[Ca^{2+}]_i$ was monitored using the fluorescent probe fluo-3 as described previously (Kawanabe et al., 2001).

MTT assay. Cells were seeded into 96-well plates at 5×10^3 cells/well for the assay using 3-(4,5-dimethyl-2-thiazolyl)-2,5-diphenyl tetrazolium bromide (MTT). They were incubated overnight in Ham's F12 medium supplemented with 10% fetal calf serum at 37°C. The cells were deprived of serum for 24 h, washed with phosphate-buffered saline, and incubated with ET-1 for a further 48 h in serum-free Ham's F12 medium with or without Ca^{2+} channel blockers. MTT assay was performed as described previously (Kawanabe et al., 2002a).

Drugs. LOE 908 was kindly provided by Boehringer Ingelheim K.G. (Ingelheim, Germany). Other chemicals were commercially obtained from the following sources: ET-1 from Peptide Institute (Osaka, Japan); SK&F 96365 from Biomol (Plymouth Meeting, PA); fluo-3/acetoxymethyl ester from Dojindo Laboratories (Kumamoto, Japan); wortmannin from Wako (Osaka, Japan); and MTT and LY 294002 from Sigma-Aldrich (St. Louis, MO)

Statistical analysis. All results were expressed as mean ± S.E.M.

Results

Effects of Wortmannin on the ET-1–Induced Increase in $[Ca^{2+}]_i$ in CHO-ET_AR. ET-1 at 10 nM induced a biphasic increase in $[Ca^{2+}]_i$ consisting of an initial transient peak and a subsequent sustained increase in both CHO-ET_AR and CHO-ET_AR preincubated with wortmannin (Fig. 1, A and B). The magnitude of the transient peak and that of the sustained increase in $[Ca^{2+}]_i$ depended on the concentration of ET-1 (Fig. 1, C and D). In experiments performed on cells incubated in a bath in which the extracellular Ca^{2+} had been removed, the transient peak was not affected on treatment with 10 nM ET-1, but the sustained increase was abolished (data not shown). The EC_{50} values (~1 nM) and the maximal effective concentration (10 nM) of ET-1 for transient increase in $[Ca^{2+}]_i$ in CHO-ET_AR preincubated with 1 μM wortmannin was similar to those in CHO-ET_AR (Fig. 1C). On the other hand, the magnitude of sustained increase in $[Ca^{2+}]_i$ caused by 10 nM ET-1 in CHO-ET_AR preincubated with wortmannin was ~20% of that in CHO-ET_AR (Fig. 1D). In contrast, addition of wortmannin after stimulation with ET-1 did not affect the sustained increase in $[Ca^{2+}]_i$ (Fig. 1A).

In CHO-ET_AR, wortmannin inhibited ET-1–induced sustained increase in $[Ca^{2+}]_i$ in a concentration-dependent manner with an IC_{50} values of ~30 nM, and maximal inhibition (~80% of control) was seen at concentrations ≥1 μM (Fig. 2, A and C). In contrast, wortmannin up to 1 μM failed to suppress ET-1–induced transient increase in $[Ca^{2+}]_i$ (Fig. 2, A and B).

Effects of LY 294002 on the ET-1–Induced Increase in $[Ca^{2+}]_i$ in CHO-ET_AR. We also used LY 294002 to evaluate

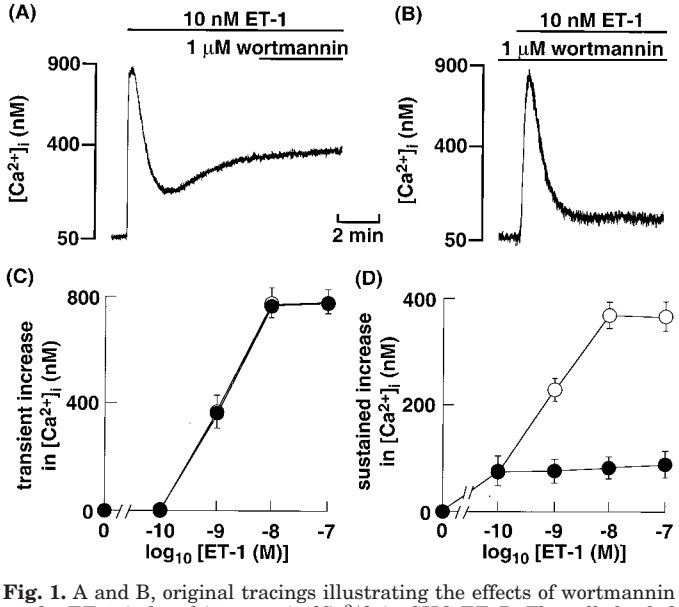

Fig. 1. A and B, original tracings illustrating the effects of wortmannin on the ET-1–induced increase in $[Ca^{2+}]_i$ in CHO-ET_AR. The cells loaded with fluo-3 were incubated with 1 μM wortmannin after (A) or before (B) 10 nM ET-1 stimulation. C and D, effects of wortmannin on the ET-1–induced transient (C) and sustained (D) increase in $[Ca^{2+}]_i$ in CHO-ET_AR. The cells loaded with fluo-3 were incubated with (●) or without (○) 1 μM wortmannin before stimulation with various concentrations of ET-1. Each point represents the mean ± S.E.M. of five experiments.

the effects of PI3K on ET-1–induced extracellular Ca^{2+} influx. LY 294002 at 50 μM inhibited PI3K activation completely in CHO cells (Kurashima et al., 1998). The magnitudes of ET-1–induced transient increase in $[Ca^{2+}]_i$ in CHO-ET_AR preincubated with 50 μM LY 294002 were similar to those in CHO-ET_AR (Fig. 3, B and C). On the other hand, 50 μM LY 294002 inhibited ET-1–induced sustained increase in $[Ca^{2+}]_i$, and ~80% inhibition was obtained (Fig. 3, B and D). Moreover, addition of LY 294002 after stimulation with ET-1 did not affect the sustained increase in $[Ca^{2+}]_i$ (Fig. 3A).

Effects of SK&F 96365 and LOE 908 on ET-1–Induced Sustained Increase in $[Ca^{2+}]_i$ in CHO-ET_AR Preincubated with Wortmannin. The ET-1–induced sustained increase in $[Ca^{2+}]_i$ in CHO-ET_AR preincubated with 1 μM wortmannin was inhibited by LOE 908 in a concentration-dependent manner, and complete inhibition was observed at concentrations ≥10 μM (Fig. 4). In contrast, SK&F 96365 up to 10 μM failed to inhibit ET-1–induced sustained increase in $[Ca^{2+}]_i$ in CHO-ET_AR preincubated with 1 μM wortmannin (Fig. 4). These results suggest that NSCC-1 is activated by ET-1 via wortmannin-independent pathway, whereas NSCC-2 and SOCC are activated via wortmannin-dependent pathway. In CHO-ET_AR preincubated with 50 μM LY 294002, ET-1–induced sustained increase in $[Ca^{2+}]_i$ was also sensitive to LOE 908 and resistant to SK&F 96365 (data not shown).

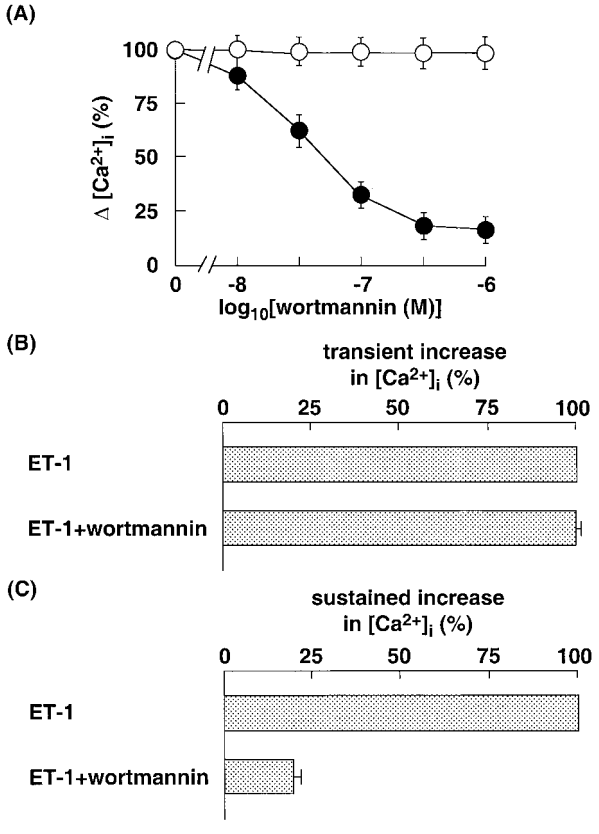

Fig. 2. A, effects of various concentrations of wortmannin on the ET-1–induced transient (○) and sustained (●) increase in $[Ca^{2+}]_i$ in CHO-ET_AR. B and C, effects of maximal concentration (1 μM) of wortmannin on the ET-1–induced transient (B) and sustained (C) increase in $[Ca^{2+}]_i$ in CHO-ET_AR. The transient and sustained increase in $[Ca^{2+}]_i$ in CHO-ET_AR in the presence of wortmannin are presented as a percentage of values in its absence. Each point represents the mean ± S.E.M. of five experiments.

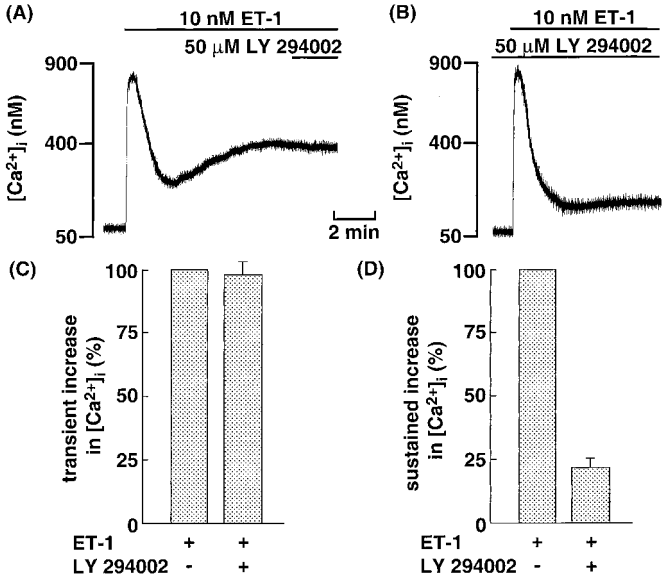

Fig. 3. A and B, original tracings illustrating the effects of LY 294002 on the ET-1–induced increase in $[Ca^{2+}]_i$ in CHO-ET_AR. The cells loaded with fluo-3 were incubated with 50 μM LY 294002 after (A) or before (B) 10 nM ET-1 stimulation. C and D, effects of 50 μM LY 294002 on the ET-1–induced transient (C) and sustained (D) increase in $[Ca^{2+}]_i$ in CHO-ET_AR. The transient and sustained increase in $[Ca^{2+}]_i$ in CHO-ET_AR in the presence of LY 294002 are presented as a percentage of values in its absence. Each point represents the mean ± S.E.M. of five experiments.

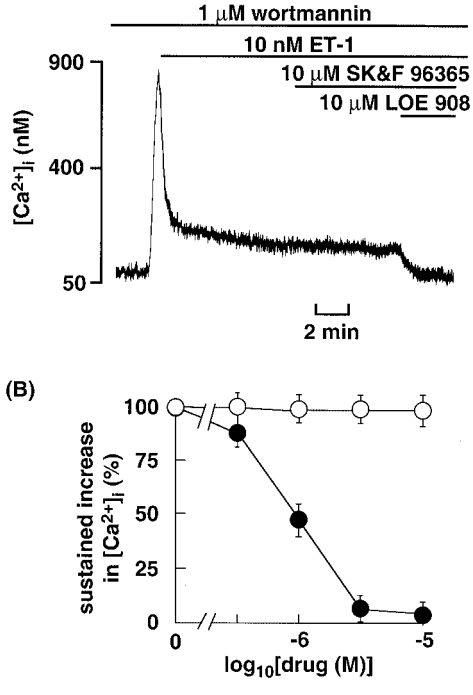

Fig. 4. A, original tracings illustrating the effects of SK&F 96365 and LOE 908 on the ET-1–induced sustained increase in $[Ca^{2+}]_i$ in CHO-ET_AR pretreated with wortmannin. The cells loaded with fluo-3 were incubated with 1 μM wortmannin before 10 nM ET-1 stimulation. After $[Ca^{2+}]_i$ reached a steady-state, 10 μM SK&F 96365 or 10 μM LOE 908 was added at the time indicated by horizontal bars. B, effects of various concentrations of SK&F 96365 (○) and LOE 908 (●) on the ET-1–induced sustained increase in $[Ca^{2+}]_i$ in CHO-ET_AR pretreated with wortmannin. The sustained increases in $[Ca^{2+}]_i$ in the presence of each drug are presented as a percentage of values in its absence. Each point represents the mean ± S.E.M. of five experiments.

Effects of Wortmannin on ET-1–Induced Sustained Increase in $[Ca^{2+}]_i$ in CHO Cells Expressing Unpalmitoylated Mutant ET_AR ($SerET_AR$). To assess the effects of wortmannin on the activation of NSCC-1, we used CHO-$SerET_AR$. $SerET_AR$ is unpalmitoylated because of substitution of all the cysteine residues to serine ($Cys^{383}Cys^{385–388}$→$Ser^{383}Ser^{385–388}$) and activates only NSCC-1 (Kawanabe et al., 2002b,c). Wortmannin at 1 μM did not affect ET-1–induced sustained increase in $[Ca^{2+}]_i$ in CHO-$SerET_AR$ (Fig. 5). LOE 908 at 10 μM inhibited ET-1–induced sustained increase in $[Ca^{2+}]_i$ completely in wortmannin-treated CHO-$SerET_AR$ (Fig. 5). On the other hand, SK&F 96365 at 10 μM failed to inhibit ET-1–induced sustained increase in $[Ca^{2+}]_i$ in these cells (Fig. 5).

Effects of ET-1 on Mitogenic Response in CHO-ET_AR. After stimulation with ET-1, the number of viable cells as estimated by the MTT assay increased with time up to 48 h in CHO-ET_AR (Fig. 6A). Therefore, in subsequent experiments, the stimulation time was set at 48 h.

ET-1 stimulated a mitogenic response in CHO-ET_AR in a concentration-dependent manner. The maximal effect was obtained at concentrations ≥10 nM (Fig. 6B). In the following experiments, ET-1 was added to the incubation media at a final concentration of 10 nM to analyze the role of Ca^{2+} channels in mitogenesis in CHO-ET_AR.

Effects of SK&F 96365 and LOE 908 on ET-1–induced mitogenesis in CHO-ET_AR. Using SK&F 96365 and LOE 908, we attempted to determine the effects of Ca^{2+} influx through VICCs on the ET-1–induced mitogenic response in CHO-ET_AR. SK&F 96365 inhibited ET-1–induced mitogenesis in a concentration-dependent manner with an IC_{50} value of ~3 μM. Maximal inhibition was observed at concentrations ≥10 μM (Fig. 7A). The extent of maximal inhibition was ~80% (Fig. 7B). Similarly, the IC_{50} values of LOE 908 for inhibition of ET-1–induced mitogenesis were ~3 μM, and maximal inhibition was observed at concentrations ≥10 μM (Fig. 7A). The extent of maximal inhibition was ~60% (Fig. 7B). Notably, the ET-1–induced mitogenesis was abolished by combined treatment with the maximally effective concentration (10 μM) of LOE 908 and SK&F 96365 (Fig. 7B). In contrast, neither SK&F 96365 nor LOE 908 had any effects at concentrations up to 30 μM on the number of cells in the absence of ET-1 (Fig. 7A).

Effects of Wortmannin on ET-1–Induced Mitogenesis in CHO-ET_AR. Wortmannin inhibited ET-1–induced mitogenesis in a concentration-dependent manner with an IC_{50} value of ~30 nM. Maximal inhibition was observed at concentrations ≥1 μM (Fig. 8A). The extent of maximal inhibition was ~80% (Fig. 8B). The wortmannin-resistant part of mitogenesis caused by ET-1 was abolished by 10 μM LOE 908 (Fig. 8B). In contrast, SK&F 96365 up to 10 μM did not affect the wortmannin-resistant part of mitogenesis caused by ET-1 (Fig. 8B).

Discussion

It is important to reveal the intracellular activation mechanisms of VICCs by ET-1. In this study, we focused on the effects of PI3K on these Ca^{2+} channels activation caused by ET-1 in CHO-ET_AR because PI3K plays important roles for stimulation of extracellular Ca^{2+} influx. Given that addition of wortmannin or LY 294002 after stimulation with ET-1 did

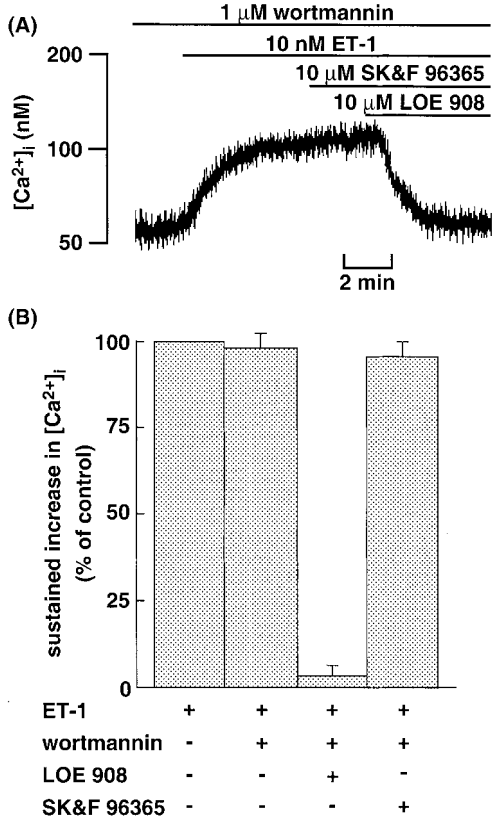

Fig. 5. A, original tracings illustrating the effects of SK&F 96365 and LOE 908 on the ET-1–induced sustained increase in $[Ca^{2+}]_i$ in CHO-$SerET_AR$ pretreated with wortmannin. The cells loaded with fluo-3 were incubated with 1 μM wortmannin before 10 nM ET-1 stimulation. After $[Ca^{2+}]_i$ reached a steady-state, 10 μM SK&F 96365 or 10 μM LOE 908 was added at the time indicated by horizontal bars. B, effects of wortmannin (1 μM), SK&F 96365 (10 μM), and/or LOE 908 (10 μM) on the ET-1–induced sustained increase in $[Ca^{2+}]_i$ in CHO-$SerET_AR$. The sustained increases in $[Ca^{2+}]_i$ in the presence of each drug are presented as a percentage of values in its absence. Data are presented as mean ± S.E.M. of five experiments.

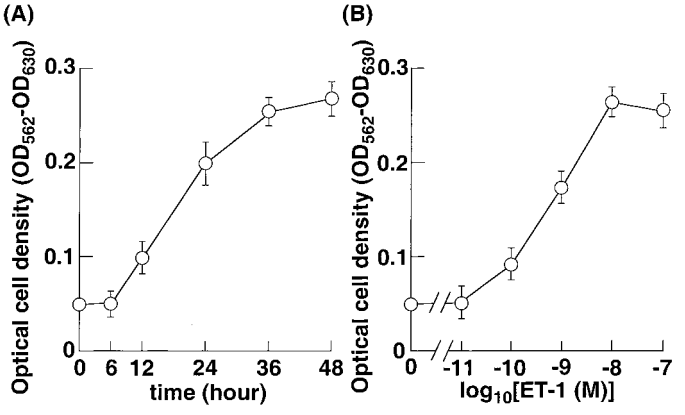

Fig. 6. A, time course of the mitogenic response of CHO-ET_AR following stimulation with ET-1. After cells had been cultured in serum-free medium for 24 h, they were stimulated with 10 nM ET-1 for the indicated time. Four hours before the end of the incubation with ET-1, MTT was added to the incubation medium to estimate the number of viable cells. B, effects of various concentrations of ET-1 on the number of viable cells in CHO-ET_AR. After cells had been deprived of serum for 24 h, they were stimulated with increasing concentrations of ET-1 for a further 48 h. Data are presented as mean ± S.E.M. of three determinations, each done in triplicate.

not suppress sustained increase in $[Ca^{2+}]_i$ (Figs. 1A and 3A), wortmannin and LY 294002 seem not to have functions as Ca^{2+} channel blockers. Therefore, wortmannin and LY 294002 may be effectors for intracellular mechanisms involved in Ca^{2+} channel activation by ET-1. Moreover, PI3K seems to be required for the activation of the Ca^{2+} entry, but not for its maintenance. The inhibitory effects of wortmannin on ET-1–induced sustained increase in $[Ca^{2+}]_i$ may be due to its inhibitory effects on PI3K, judging from the following data: 1) Wortmannin is generally accepted as a PI3K inhibitor (Ui et al., 1995). Moreover, at nanomolar concentrations, wortmannin acts specifically on PI3K (Yano et al., 1993). 2) Another PI3K inhibitor, LY 294002, also inhibited the wortmannin-sensitive part of ET-1–induced sustained increase in $[Ca^{2+}]_i$. 3) In CHO-ET_AR, the IC_{50} values (~30 nM) and maximal effective concentration (1 μM) of wortmannin for ET-1–induced sustained increase in $[Ca^{2+}]_i$ (Fig. 2) were similar to those for ET-1–induced phosphatidylinositol triphosphate formation as an index of PI3K activity (Sugawara et al., 1996).

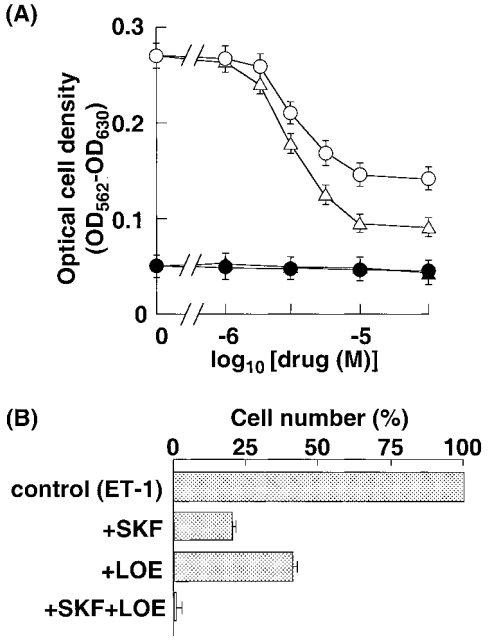

Fig. 7. A, effects of various concentrations of SK&F 96365 and LOE 908 on the ET-1–induced mitogenic response in CHO-ET_AR. Starved cells were incubated for 15 min with increasing concentrations of SK&F 96365 (triangles) or LOE 908 (circles), and then they were stimulated with (open symbols) or without (closed symbols) 10 nM endothelin-1. B, effects of a maximally effective concentration of SK&F 96365 (10 μM) and/or LOE 908 (10 μM) on the ET-1–induced mitogenic response. The ET-1–induced mitogenic responses in the presence of SK&F 96365 and/or LOE 908 are represented as a percentage of values in its absence. Data are presented as mean ± S.E.M. of three experiments.

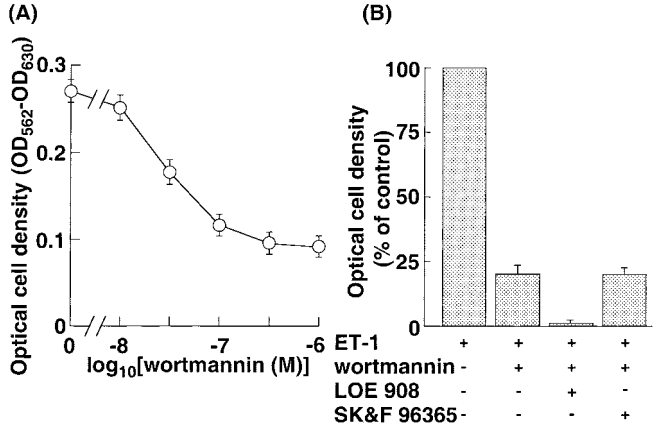

Fig. 8. A, effects of various concentrations of wortmannin on the ET-1–induced mitogenic response in CHO-ET_AR. Starved cells were incubated for 15 min with increasing concentrations of wortmannin, and then they were stimulated with 10 nM ET-1. B, effects of a maximally effective concentration of wortmannin (1 μM), SK&F 96365 (10 μM), and/or LOE 908 (10 μM) on the ET-1–induced mitogenic response. The ET-1–induced mitogenic response in the presence of wortmannin, SK&F 96365, and/or LOE 908 are represented as a percentage of values in its absence. Data are presented as mean ± S.E.M. of three experiments.

Because wortmannin partially suppressed ET-1–induced sustained increase in $[Ca^{2+}]_i$ (Figs. 1 and 2), ET-1 induces extracellular Ca^{2+} influx through VICCs via both PI3K-dependent and -independent pathways in CHO-ET_AR. Based on the sensitivity to SK&F 96365 and LOE 908, the wortmannin-resistant part of sustained increase in $[Ca^{2+}]_i$ was caused by Ca^{2+} influx through NSCC-1 (LOE 908-sensitive and SK&F 96365-resistant) (Fig. 4). Therefore, Ca^{2+} influx through NSCC-2 and SOCC are composed of wortmannin sensitive part. These results indicate that PI3K may play important roles for ET-1–induced activation of NSCC-2 and SOCC. The result that wortmannin failed to inhibit the activation of NSCC-1 by ET-1 in CHO-SerET_AR (Fig. 5) is consistent with this indication. Both NSCC-2 and SOCC activations by ET-1 involve G_q/PLC-dependent cascade and depend on mobilization of Ca^{2+} from the intracellular Ca^{2+} store in CHO-ET_AR (Kawanabe et al., 2002c). Moreover, it is generally accepted that $G_{\beta\gamma}$ is involved in PI3K activation (Clapham and Neer, 1997; Vanhaesebroeck et al., 1997). Therefore, $G_{\beta\gamma}$ as well as G_α may play important roles for NSCC-2 and SOCC activation by ET-1.

ET-1 induces mitogenic response in CHO-ET_AR, judging from results of MTT assay as described previously (Sugawara et al., 1996). The inhibitory action of SK&F 96365 or LOE 908 on ET-1–induced mitogenesis may be mediated by blockade of Ca^{2+} entry through VICCs for the following reasons: the IC_{50} values of SK&F 96365 and LOE 908 for ET-1–induced mitogenesis and the extent of inhibition of the response by these blockers (Fig. 7) correlated well with those for the ET-1–induced $[Ca^{2+}]_i$ response (Kawanabe et al., 2001), and neither SK&F 96365 nor LOE 908 is considered to exert cytotoxic effects on quiescent cells, judging from data from MTT assay (Fig. 7). The ET-1–induced mitogenesis can be divided into three parts based on its pharmacology. The first part is sensitive to LOE 908 and resistant to SK&F 96365, the second is sensitive to both LOE 908 and SK&F 96365, and the third is resistant to LOE 908 and sensitive to SK&F 96365 (Fig. 7B). The pharmacological criteria indicate that the first part involves Ca^{2+} entry through NSCC-1, the second involves Ca^{2+} entry through NSCC-2, and the third involves Ca^{2+} entry through SOCC. Furthermore, the percentage contribution of Ca^{2+} entry through NSCC-1, NSCC-2, and SOCC to the mitogenesis is calculated to be 20, 40, and 40%, respectively (Fig. 7B). The inhibitory effects of wortmannin on ET-1–induced mitogenesis may be mediated by blockade of Ca^{2+} entry through NSCC-2 and SOCC for the following reasons: the IC_{50} values of wortmannin for ET-1–induced mitogenesis (Fig. 8A) correlated well with those for the ET-1–induced $[Ca^{2+}]_i$ response (Fig. 2A), and the wortmannin-resistant part of ET-1–induced mitogenesis was de-

pendent on the extracellular Ca^{2+} influx through NSCC-1, based on the sensitivity to SK&F 96365 and LOE 908 (SK&F 96365-resistant and LOE 908-sensitive) (Fig. 8B). Moreover, these results indicate that PI3K may be involved in the ET-1–induced mitogenesis by activating extracellular Ca^{2+} influx through NSCC-2 and SOCC.

In conclusion, NSCC-2 and SOCC are stimulated by ET-1 via PI3K-dependent cascade, whereas NSCC-1 is stimulated via PI3K-independent cascade. Moreover, PI3K is involved in the ET-1–induced mitogenesis that depends on the extracellular Ca^{2+} influx through SOCC and NSCC-2.

Acknowledgments

We thank Boehringer Ingelheim K.G. for the kind donation of LOE 908.

References

Clapham DE and Neer EJ (1997) G protein $\beta\gamma$ subunits. *Annu Rev Pharmacol Toxicol* **37:**167–203.

Haak T, Marz W, Jungmann E, Hausser S, Siekmeier R, Gross W, and Usadel KH (1994) Elevated endothelin levels in patients with hyperlipoproteinemia. *Clin Invest* **72:**580–584.

Hsu AL, Ching TT, Sen G, Wang DS, Bondada S, Authi KS, and Chen CS (2000) Novel function of phosphoinoitide 3-kinase in T cell Ca^{2+} signaling. *J Biol Chem* **275:**16242–16250.

Kawanabe Y, Okamoto Y, Enoki T, Hashimoto N, and Masaki T (2001) Ca^{2+} channels activated by endothelin-1 in CHO cells expressing endothelin-A or endothelin-B receptors. *Am J Physiol* **281:**C1676–C1685.

Kawanabe Y, Hashimoto N, and Masaki T (2002a) Ca^{2+} channels involved in endothelin-induced mitogenic response in carotid artery vascular smooth muscle cells. *Am J Physiol* **282:**C330–C337.

Kawanabe Y, Okamoto Y, Hashimoto N, Miwa S, and Masaki T (2002b) Molecular mechanism for endothelin-1-induced stress fiber formation: analysis of G proteins using a mutant $endothelin_A$ receptor. *Mol Pharmacol* **61:**277–284.

Kawanabe Y, Okamoto Y, Miwa S, Hashimoto N, Masaki T (2002c) Molecular mechanisms for activation of voltage-independent Ca^{2+} channels by endothelin-1 in Chinese hamster ovary cells stably expressing human $endothelin_A$ receptors. *Mol Pharmacol* **62:**75–80.

Kurashima K, Szabo EZ, Lukacs G, Orlowski J, and Grinstein S (1998) Endosomal recycling of the Na^+/H^+ exchanger NHE3 isoform is regulated by the phosphatidylinositol 3-kinase pathway. *J Biol Chem* **273:**20828–20836.

Lerman A, Edwards BS, Hallett JW, Heublein DM, Soderg SM, and Burnett JC (1991) Circulating and tissue endothelin immunoreactivity in advanced atherosclerosis. *N Engl J Med* **325:**997–1001.

Seki T, Yokoshiki H, Sunagawa M, Nakamura M, and Sperelakis N (1999) Angiotensin II stimulation of Ca^{2+}-channel current in vascular smooth muscle cells is inhibited by lavendustin-A and LY-294002. *Pflueg Arch Eur J Physiol* **437:**317–323.

Sugawara F, Ninomiya H, Okamoto Y, Miwa S, Mazda O, Katsura Y, and Masaki T (1996) Endothelin-1-induced mitogenic responses of Chinese hamster ovary cells expressing human endothelinA: the role of a wortmannin-sensitive signaling pathway. *Mol Pharmacol* **49:**447–457.

Ui M, Okada T, Hazeki K, and Hazeki O (1995) Wortmannin as a unique probe for an intracellular signalling protein, phosphoinositide 3-kinase. *Trends Biochem Sci* **20:**303–307.

Vanhaesebroeck B, Leevers SJ, Panayotou G, and Waterfield MD (1997) Phosphoinositide 3-kinases: a conserved family of signal transducers. *Trends Biochem Sci* **22:**267–272.

Viard P, Exner T, Maier U, Mironneau J, Nurnberg B, and Macrez N (1999) $G\beta\gamma$ dimers stimulate vascular L-type Ca^{2+} channels via phosphoinositide 3-kinase. *FASEB J* **13:**685–694.

Yanagisawa M, Kurihara H, Kimura S, Tomobe Y, Kobayashi M, Mitsui Y, Yazaki Y, Goto K, and Masaki T (1988) A novel vasoconstrictor peptide produced by vascular endothelial cells. *Nature (Lond)* **332:**411–415.

Yano H, Nakanishi S, Kimura K, Hanai N, Saitoh Y, Fukui Y, Nonomura Y, and Matsuda Y (1993) Inhibition of histamine secretion by wortmannin through the blockade of phosphatidyl 3-kinase in RBL-2H3 cells. *J Biol Chem* **268:**13–16.

Zhang XF, Iwamuro Y, Enoki T, Okazawa M, Lee K, Komuro T, Minowa T, Okamoto Y, Hasegawa H, Furutani H, et al. (1999) Pharmacological characterization of Ca^{2+} entry channels in endothelin-1-induced contraction of rat aorta using LOE 908 and SK&F 96365. *Br J Pharmacol* **127:**1388–1398.

Address correspondence to: Yoshifumi Kawanabe M.D., Ph.D., Membrane Biology Program, Brigham and Women's Hospital, Harvard Institutes of Medicine, Room 520, 77 Avenue Louis Pasteur, Boston, MA 02115. E-mail: ykawanabe@rics.bwh.harvard.edu